AIP | Applied Physics Letters

Time-of-flight-photoelectron emission microscopy on plasmonic structures using attosecond extreme ultraviolet pulses

S. H. Chew, F. Süßmann, C. Späth, A. Wirth, J. Schmidt et al.

Citation: Appl. Phys. Lett. **100**, 051904 (2012); doi: 10.1063/1.3670324
View online: http://dx.doi.org/10.1063/1.3670324
View Table of Contents: http://apl.aip.org/resource/1/APPLAB/v100/i5
Published by the American Institute of Physics.

Time-of-flight-photoelectron emission microscopy on plasmonic structures using attosecond extreme ultraviolet pulses

S. H. Chew (周淑芬),[1,2,a)] F. Süßmann,[2] C. Späth,[1] A. Wirth,[2] J. Schmidt,[1] S. Zherebtsov,[2] A. Guggenmos,[1,2] A. Oelsner,[3] N. Weber,[4] J. Kapaldo,[2] A. Gliserin,[1,2] M. I. Stockman,[5] M. F. Kling,[2] and U. Kleineberg[1,2]

[1]*Faculty of Physics, Ludwig Maximilian University of Munich, 85748 Garching, Germany*
[2]*Max Planck Institute of Quantum Optics, 85748 Garching, Germany*
[3]*Surface Concept GmbH, Staudingerweg 7, 55128 Mainz, Germany*
[4]*Focus GmbH, Hünstetten Kasselbach, 65510, Germany*
[5]*Department of Physics and Astronomy, Georgia State University, Atlanta 30303 USA*

(Received 18 August 2011; accepted 11 November 2011; published online 2 February 2012)

We report on the imaging of plasmonic structures by time-of-flight-photoemission electron microscopy (ToF-PEEM) in combination with extreme ultraviolet (XUV) attosecond pulses from a high harmonic generation source. Characterization of lithographically fabricated Au structures using these ultrashort XUV pulses by ToF-PEEM shows a spatial resolution of ~200 nm. Energy-filtered imaging of the secondary electrons resulting in reduced chromatic aberrations as well as microspectroscopic identification of core and valence band electronic states have been successfully proven. We also find that the fast valence band electrons are not influenced by space charge effects, which is essentially important for attosecond nanoplasmonic-field microscopy realization. © *2012 American Institute of Physics*. [doi:10.1063/1.3670324]

Surface plasmons are coherent electron excitations at metal-dielectric interfaces appearing as localized field enhancements (localized surface plasmons, LSPs) on nanoscaled metal structures or travelling plasmon excitations (surface plasmon polaritons, SPPs) in plasmonic waveguides. Intrinsically, LSPs could undergo ultrafast dynamics as short as ~100 attoseconds as defined by the inverse broad spectral bandwidth of the plasmonic resonances when excited by femtosecond few-cycle laser pulses.[1] To date, real-time observation of these nanoplasmonic fields with nanometer spatial and attosecond temporal resolution has not yet been achieved. Therefore, we proposed an approach which combines time-of-flight-photoemission electron microscopy (ToF-PEEM)[2,3] and attosecond streaking spectroscopy[4,5] to detect the spatiotemporal dynamics in an optical-pump/extreme ultraviolet (XUV)-probe scheme.[1] The basic idea is to use a few-cycle optical pulse to resonantly drive the nanoplasmonic fields on a nanostructured metal surface, while a synchronized attosecond XUV pulse with a variable time delay is then sent to the system to probe the fields. This is performed via the liberated photoelectrons from the surface, which are spatially and spectroscopically detected by a ToF-PEEM. Photoelectron streaking of the liberated fast valence band electrons in the plasmonic near fields results in a kinetic energy shift of some eV, which is directly detectable only in ToF-PEEM. We previously showed that ~50 meV energy resolution and ~25 nm spatial resolution could be achieved with our ToF-PEEM setup in a threshold photoemission mode using ultraviolet (UV) excitation.[6]

Following the described atto-PEEM concept, we here experimentally demonstrate a spatial resolution of ~200 nm obtained from Au plasmonic structures by a low repetition rate (1 kHz) pulsed attosecond XUV excitation in medium magnification PEEM mode. Energy-filtered imaging was performed to improve the image contrast acquired from secondary electrons particularly in ToF mode when a larger contrast aperture in the back-focal plane was used. We show that the resulting photoelectron spectra depend on the local chemical composition of the nanostructured sample surface. We also demonstrate the dependence of image blurriness and spectral shift as well as broadening on the XUV intensity due to space charge effects. We further observe a significantly high count rate of fast direct Au-5d valence band electrons emitted from the Au surface which carry the attosecond temporal information imprinted during the attosecond pulsed photoexcitation, and the ultrashort escape time of these electrons from the surface allows "frozen snapshots" of ultrafast nanoplasmonic fields to be recorded in an optical pump-XUV probe experiment.[1]

The experimental scheme is depicted in Fig. 1. The 1 kHz attosecond XUV pulses are produced via high harmonic generation (HHG) by ionizing neon atoms with waveform-controlled near-infrared (NIR) laser pulses of ~0.5 mJ energy and 5 fs duration from a Ti:Sapphire amplifier system. The NIR beam is blocked by a 150 nm Zr while the XUV beam is spectrally and spatially filtered by a 150 nm Si_3N_4 filter and an iris. The resulting XUV spectrum peaks at 97 eV after being filtered by the Zr and Si_3N_4 filters, as measured by an XUV flatfield spectrograph (see inset in Fig. 1). The XUV beam is further spectrally filtered at around 93 eV and focused onto the sample in the ToF-PEEM by means of a concave Mo/Si multilayer mirror of 12.5 cm focal length. The 5.4 eV full width at half maximum (FWHM) spectral bandwidth of the mirror reflectivity supports XUV pulses with a Fourier limit of ~350 as. The incidence angle of the p-polarized XUV beam is 65° to the sample surface normal. 3D (x, y, t) datasets of the lateral and energy distribution of the photoelectrons via time-of-flight

a)Electronic mail: SooHoon.Chew@physik.uni-muenchen.de.

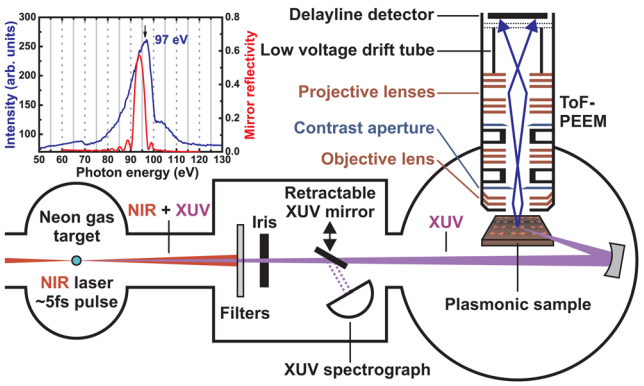

FIG. 1. (Color online) Schematic view of the experimental setup. Inset: the XUV spectrum filtered by Zr and Si_3N_4 filters is plotted together with the simulated XUV mirror's reflectivity peaked at 93 eV with a bandwidth of 5.4 eV.

measurements are acquired by the ToF-PEEM (Ref. 6) in combination with a 2D delayline detector (DLD).[7]

The first Au plasmonic structures on Si wafer substrates with native oxide coverage we used in the experiments were fabricated by electron beam lithography (EBL) and ion beam etching. This chessboard sample consists of alternating 1 μm × 1 μm Au squares of a layer thickness of 100 nm. A 15 nm thick Cr layer was added between the Au layer and the Si substrate as an adhesion layer to improve the quality of Au layer. In the first series of PEEM imaging, a high drift voltage of 130 V was applied in the drift tube (without ToF option). The extractor voltage of the PEEM objective lens was set to 20 kV (medium magnification mode) and a back-focal contrast aperture of 150 μm was chosen. Fig. 2(a) shows the PEEM image of the Au square sample excited by a 4.9 eV Hg arc UV lamp. The spatial resolution is estimated by taking the intensity profile over the structure edge region (averaging over the 1 μm edge length) following a 16%–84% criterion error function fit. By averaging five intensity profiles from different sample positions, we estimate a spatial resolution of 153 ± 10 nm for the UV-PEEM image. Fig. 2(b) depicts the PEEM image of the same sample which is excited by XUV attosecond pulses of 93 eV photon energy. The estimated spatial resolution for the XUV-PEEM image is 194 ± 50 nm (average from five different sample positions). The images in Figs. 2–4 are flat-field corrected for DLD gain. It is to be pointed out that several hot spots on the sample indicated by the very bright areas in the XUV image are induced by the nanoplasmonic fields due to NIR leakage through the pinholes of the filters. The inhomogeneous illumination on the sample by XUV excitation is mainly contributed by the beam profile and filter structure. The XUV-PEEM image is typically of lower contrast in comparison to the UV-PEEM image, attributing to vanishing work function contrast and broader electron energy spectrum for the 93 eV XUV excitation. The XUV pulse intensity was reduced by decreasing the neon gas pressure to avoid the space charge effect that causes image blurriness.[8] This required decrease in XUV intensity currently limits the ability to achieve imaging in high resolution PEEM mode where the transmission of photoelectrons is drastically decreased. However, this can be overcome by an increase in pulse repetition rate from 1 kHz to 10 kHz in a next generation setup.

In the second series of PEEM imaging, a low drift voltage of 40 V was applied in the drift tube (with ToF option) to disperse the electrons in time. The PEEM extractor voltage was again set to 20 kV and the largest contrast aperture of 1500 μm was used to increase the transmission of higher energy photoelectrons. However, the PEEM resolution is now reduced due to spherical and chromatic aberrations of the objective lens as a consequence of a larger contrast aperture size. Fig. 3 illustrates the electron energy spectrum excited by XUV which is spatially integrated over the whole sample area as depicted in the left inset. The spectrum, which is corrected for the work function difference between the sample surface and the drift tube, exhibits basically two peaks, at low energy (true secondary electrons) and at high energy (primary valence band electrons). The maximum kinetic electron energy (valence band electrons at the Fermi edge) detected, corresponds to the central XUV photon energy of 93 eV, reduced by the material work function (5.1 eV for polycrystalline Au (Ref. 9) and 4.5 eV for amorphous SiO_2 (Ref. 10)). By selecting a narrow energy interval ΔE, in this case of 1–3 eV within the secondary electron peak, the image contrast has been significantly enhanced due to a smaller energy spread, as illustrated in the right inset of Fig. 3. However, the spatial resolution in ToF mode with the largest contrast aperture has now degraded to ~300 nm as compared to without ToF mode. Energy-filtered imaging using the high energy valence band electron distribution at ~83 eV can be performed similarly; however Au and SiO_2 show a very similar valence band electron yield at 93 eV photon excitation (see section below) and thus do not provide sufficient image contrast.

In order to separate the spectroscopic contributions of the Au and SiO_2 areas of the sample, we have performed microspectroscopic investigations on selected areas of Au

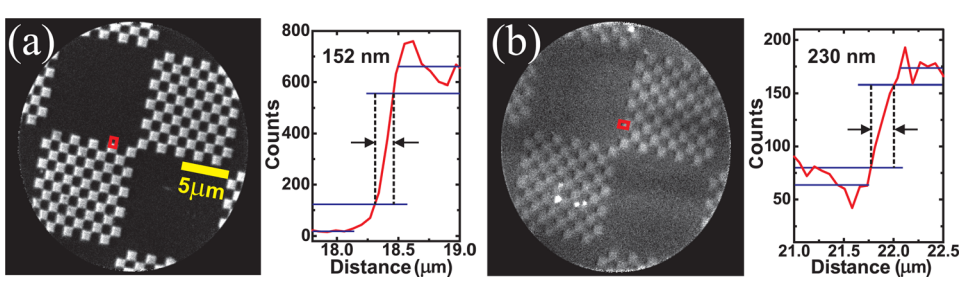

FIG. 2. (Color online) (a) Left: UV-PEEM image of Au squares illuminated by an Hg arc lamp with an exposure time of 2 min; and right: exemplary intensity profile extracted from the region marked on the image in (a) gives a spatial resolution of 152 nm. (b) Left: XUV-PEEM image illuminated by XUV attosecond pulses under the same conditions with an exposure time of 1.5 h; and right: exemplary intensity profile extracted from the region marked on the image in (b) gives a spatial resolution of 230 nm.

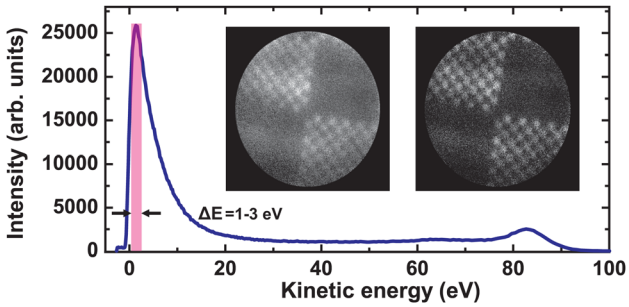

FIG. 3. (Color online) Full energy spectrum of XUV excited photoelectrons integrated over the whole Au sample area as shown in the left inset. Left inset: integrated image of XUV excitation over the full electron energy spectrum with an exposure time of 1.5 h. Right inset: energy-selective image in the range of 1–3 eV of the secondary electron peak from XUV excitation.

ellipsoid nanostructures on a Si wafer with native oxide coverage. The 500 nm gap Au ellipsoid sample (Au layer thickness = 20 nm and Cr layer thickness = 4 nm) was fabricated by EBL and lift-off. Fig. 4(a) shows the UV-PEEM image with Hg lamp excitation. The integrated XUV-PEEM image together with the spatially resolved spectra are displayed in Figs. 4(b) and 4(c). We identified three distinctly different image areas with the corresponding spectra. A prominent 5d valence band of Au is observed below the Fermi edge.[11] However, the fine structure of this Au-5d band cannot be resolved due to the broad spectral bandwidth of the XUV pulses. Furthermore, an O(2s) peak is seen on the SiO_2 area besides the p-type Si valence band photoemission.[12] A very high electron count rate from the hot spot area with a smaller energetic width than the XUV induced secondary electron distribution is attributed to multiphoton processes and nanolocalized field enhancement due to NIR leakage onto the sample [see Fig. 4(c)].

Space charge effects in photoemission are frequently observed when using ultrashort laser pulse systems of pulse durations ranging from femtoseconds to attoseconds.[8,13,14] Here, we analyze the space charge effects on image quality and electron spectra with attosecond XUV pulses. Fig. 5(a) shows a series of XUV-PEEM images on the same chessboard sample at different neon gas pressures with an exposure time of 10 min for each image. The XUV intensity is increased by raising the gas pressure. Fig. 5(b) displays the corresponding spectra varying with the gas pressure. The image starts to get blurred at a pressure of 70 mbar [see Fig. 5(a)], whereas the spectrum only starts to get broadened at 80 mbar [see Fig. 5(b)]. Considering the transmission function of the PEEM for the given contrast aperture, we estimate an electron flux from the sample of ~13 e/sμm^2 at 70 mbar. Note that the very bright spot in the top area of the image at 90 mbar and 100 mbar can be an artifact resulting from multiple hits on the DLD in addition to the blurriness caused by the space charge effect. This can be explained by a count rate of more than 1000 events per second at the DLD at 90 mbar and 100 mbar. Interestingly, it is observed that the high energy electron peaks do not shift in energy as the gas pressure increases. On the other hand, the low energy electron peak starts to shift at 90 mbar from 1.4 eV to 3.7 eV. At 100 mbar, the energy is shifted to 5.5 eV. This shows that the low energy electrons (secondary electrons) are more easily influenced by space charge effects as they are slow compared to the high energy valence band electrons. Hence, the atto-PEEM concept can be realized using the fast valence band electrons, since they are hardly affected by space charge effects even at the current 1 kHz XUV source.

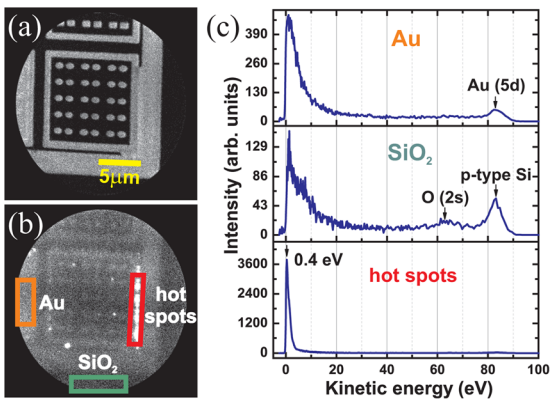

FIG. 4. (Color online) (a) UV-PEEM image of 500 nm gap Au ellipsoids illuminated by an Hg arc lamp with an exposure time of 5 min. (b) XUV-PEEM image illuminated by XUV attosecond pulses under the same conditions with an exposure time of 1 h. Three different regions (Au, SiO_2, and hot spots) on the sample are selected for microspectroscopy. (c) The corresponding spectra of the three marked regions shown in (b).

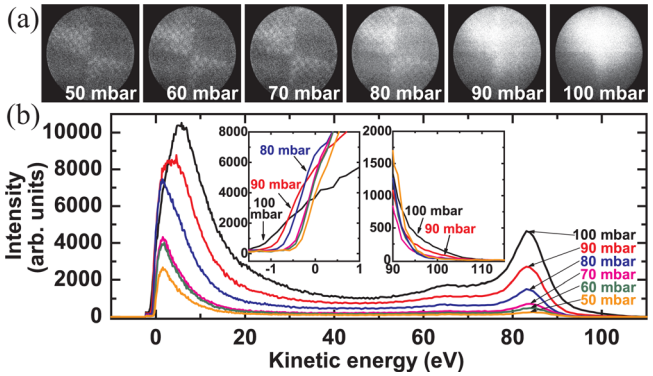

FIG. 5. (Color online) (a) PEEM images excited by XUV at different gas pressures in mbar. (b) The full energy spectra of XUV emitted photoelectrons at different gas pressures in mbar. Left inset: intensity normalized at secondary electron peak. Right Inset: intensity normalized at primary electron peak.

The experimental results demonstrate next steps toward the temporal characterization of nanoscaled LSPs in a femtosecond optical-pump/attosecond XUV-probe experiments. Energy-filtered imaging of fast valence band electrons and spatial resolution down to 100 nm using attosecond pulses can be realized with a higher magnification mode of the PEEM (using the highest extractor voltage of 30 kV) and a currently under development 10 kHz repetition rate XUV source in our laboratory.

We acknowledge gratefully the financial support by the BES Office of the U.S. Department of Energy, German Science Foundation (DFG) through the Emmy-Noether program, the Cluster of Excellence: Munich Centre for Advanced Photonics, the priority program SPP 1391, and the BMBF via PhoNa. J.K. acknowledges support by the DAAD through the RISE program. We acknowledge F. Krausz, A. Mikkelsen, and C. Schneider for fruitful discussions. We are

also grateful to J. Lin, S. Watson, S. Trushin, and M. Hofstetter for their contributions to the experimental setup.

[1]M. I. Stockman, M. F. Kling, U. Kleineberg, and F. Krausz, Nat. Photonics **1**, 539 (2007).
[2]H. Spiecker, O. Schmidt, C. Ziethen, D. Menke, U. Kleineberg, R. C. Ahuja, M. Merkel, U. Heinzmann, and G. Schnönhense, Nucl. Instrum. Methods Phys. Res. A **406**, 499 (1998).
[3]A. Oelsner, M. Rohmer, C. Schneider, D. Bayer, G. Schnönhense, and M. Aeschlimann, J. Electron Spectrosc. Relat. Phenom. **178–179**, 317 (2010).
[4]R. Kienberger, E. Goulielmakis, M. Uiberacker, A. Baltuska, V. Yakovlev, F. Bammer, A. Scrinzi, T. Westerwalbesloh, U. Kleineberg, U. Heinzmann, M. Drescher, and F. Krausz, Nature **427**, 817 (2004).
[5]P. B. Corkum and F. Krausz, Nat. Phys **3**, 381 (2007).
[6]J. Lin, N. Weber, A. Wirth, S. H. Chew, M. Escher, M. Merkel, M. F. Kling, M. I. Stockman, F. Krausz, and U. Kleineberg, J. Phys.: Condens. Matter **21**, 314005 (2009).
[7]A. Oelsner, A. Krasyuk, G. H. Fecher, C. M. Schneider, and G. Schnönhense, J. Electron Spectrosc. Relat. Phenom. **137–140**, 757 (2004).
[8]A. Mikkelsen, J. Schwenke, T. Fordell, G. Luo, K. Klünder, E. Hilner, N. Anttu, A. A. Zakharov, E. Lundgren, J. Mauritsson *et al*., Rev. Sci. Instrum. **80**, 123703 (2009).
[9]R. J. C. Batista, M. S. C. Mazzoni, and H. Chacham, Nanotechnology **21**, 065705 (2010).
[10]T. Seldrum, R. Bommena, L. Samain, J. Dumont, S. Sivananthan, and R. Sporken, J. Vac. Sci. Technol. B **26**, 1105 (2008).
[11]N. V. Smith, G. K. Wertheim, S. Hüfner, and M. M. Traum, Phys. Rev. B **10**, 3197 (1974).
[12]J. L. Alay, M. Fukuda, C. H. Bjorkman, K. Nakagawa, S. Yokoyama, S. Sasaki, and M. Hirose, Jpn. J. Appl. Phys. **34**, L653 (1995).
[13]N. M. Buckanie, J. Göhre, P. Zhou, D. von der Linde, M. H. von Hoegen, and F.-J. M. zu Heringdorf, J. Phys.: Condens. Matter **21**, 314003 (2009).
[14]S. Passlack, S. Mathias, O. Andreyev, D. Mittnacht, M. Aeschlimann, and M. Bauer, J. Appl. Phys. **100**, 024912 (2006).